Synthesis and Characterization of $Rb_2(MoO_2)_3(As_2O_7)_2 \cdot 2H_2O$: The First Rubidium Molybdenum(VI) Diarsenate with a Porous Structure

Kuei-Fang Hsu and Sue-Lein Wang*

Department of Chemistry, National Tsing Hua University, Hsinchu 300, Taiwan

Received March 14, 2000

Introduction

Microporous materials containing transition metal elements are a focus of contemporary research[1] due to their novel potential catalytic, electrical, optical, and magnetic properties which are not accessible to the main group systems of tetrahedral framework zeolites. In the past decade, the microporous behavior was successfully extended into the phosphate and arsenate systems of titanium, vanadium, manganese, iron, cobalt, copper, and molybdenum.[2,3] The synthetic strategy usually involved the combination of mild hydrothermal conditions to avoid yielding dense phases with organic templates for generating cages or channels. Recently open-framework solids with extremely low framework-metal-atom density (FD) were obtained by employing inorganic cations.[3] We have been interested in the synthesis of microporous materials using large inorganic cations as structural-directing reagents.[4−7] However, employing low temperatures had often led to low-dimensional polyoxomolybdate anion structures in the $Mo^{VI}/As^{V}/O$ system.[5,6] High-temperature hydrothermal routes had been tried and were once successful in the alkaline-earth metal cation system where a porous solid, $Ba_3(MoO_3)_3(H_2O)(AsO_4)_2$[7] (FD = 13.1 M atoms/1000 Å^3), the first extended lattice containing *anti*-Lipscomb facial $\{MoO_3\}$ units, was prepared. Further explorations of high-temperature routes via the flux-growth method at 600 °C yielded a more porous solid, $Cs_2Mo_2O_5As_2O_7 \cdot H_2O$[6] (FD = 12.0 M atoms/1000 Å^3), which has been the most open and stable metal diarsenate framework ever reported.

Reports on multidimensional extended structures in the ternary molybdenum(VI) diarsenate system is very limited. The only examples include the layered $K_2MoO_2As_2O_7$[8] and the tunneled $K_2MoO_2(MoO_2As_2O_7)_2$[9] and $Cs_2Mo_2O_5As_2O_7 \cdot H_2O$.[6] Driven by the curiosity of structural versatility as well as to complete the series of alkaline metal cations, we have extended the flux methods to the unexplored Rb system.[7] Herein, we report the first rubidium molybdenum(VI) diarsenate phase, Rb_2-

Table 1. Crystallographic Data

empirical formula	$H_4As_4Mo_3O_{22}Rb_2$	Z	4
space group	$C2/c$	ρ_{calcd}, g cm^{-3}	3.791
a, Å	21.0215(9)	μ, mm^{-1}	13.684
b, Å	9.8341(4)	λ, Å	0.71073
c, Å	9.5223(4)	T, °C	23
β, deg	97.292(1)	R1[a]	0.0353
V, Å^3	1952.6(1)	wR2[b]	0.0908

[a] $R1 = \sum||F_o| - |F_c||/\sum|F_o|$. [b] $wR2 = \sum w(F_o^2 - F_c^2)^2/\sum[w(F_o^2)^2]^{1/2}$, $w = [\sigma_2(Fo) + (0.0578P)^2 + 4.4516P]^{-1}$, where $P = (F_o^2 + 2F_c^2)/3$.

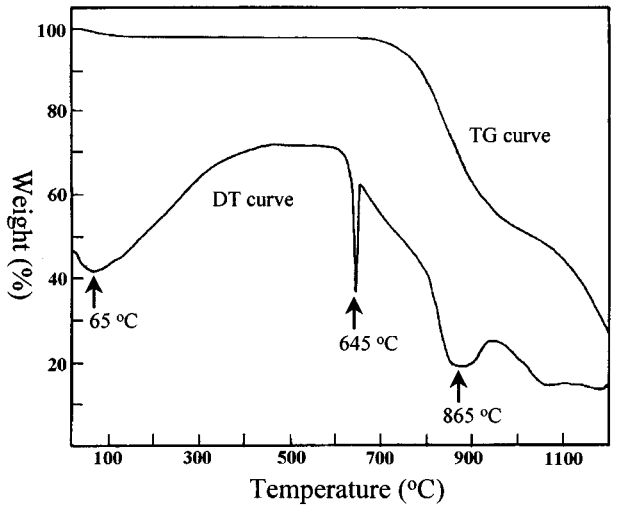

Figure 1. TGA and DTA curves of $Rb_2(MoO_2)_3(As_2O_7)_2 \cdot 2H_2O$ (**1**).

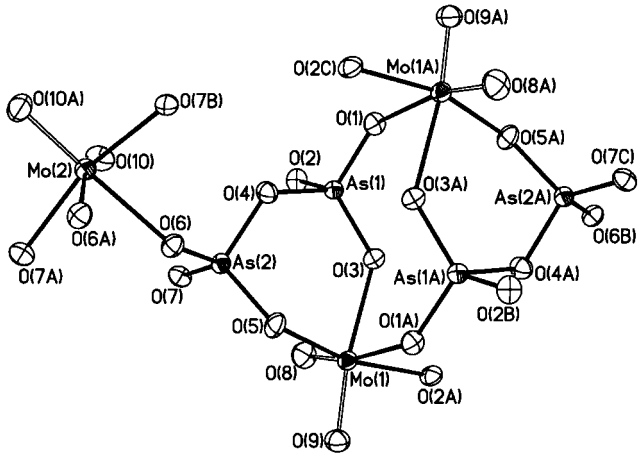

Figure 2. ORTEP drawing of the asymmetric unit in structure **1**. Thermal ellipsoids are given at the 50% level.

* Author to whom correspondence should be addressed. E-mail: slwang@mx.nthu.edu.tw. Tel: 886-35-721074. Fax: 886-35-711082.

(1) (a) Cheetham, A. K.; Férey, G.; Loiseau, T. *Angew. Chem., Int. Ed.* **1999**, *38*, 3268. (b) Huang, Q.; Ulutagay, M.; Michener, P. A.; Hwu, S. J. *J. Am. Chem. Soc.* **1999**, *121*, 10323. (c) Bu, X.; Feng, P.; Stucky, G. D. *Science* **1997**, *278*, 2080. (d) Feng, P.; Bu, X.; Stucky, G. D. *Nature* **1997**, *388*, 735. (e) Gier, T. E.; Bu, X.; Wang, S. L.; Stucky, G. D. *J. Am. Chem. Soc.* **1996**, *118*, 3039. (f) Zubieta, J. *Comments Inorg. Chem.* **1994**, *16*, 153. (g) Clearfield, A. *Comments Inorg. Chem.* **1990**, *10*, 89.

(2) (a) Xu, Y. *Curr. Opin. Solid State Mater. Sci.* **1999**, *4*, 133. (b) Lii, K. H.; Huang, Y. F.; Zima, V.; Huang, C. Y.; Lin, H. M.; Jiang, Y. C.; Liao, F. L.; Wang, S. L. *Chem. Mater.* **1998**, *10*, 2599. (c) Lii, K. H. *Inorg. Chem.* **1995**, *34*, 1700. (d) Wang, S. L.; Lee, Y. H. *Inorg. Chem.* **1994**, *33*, 3845. (e) Guesdon, A.; Borel, M. M.; Leclaire, A.; Grandin, A.; Raveau, B. *J. Solid State Chem.* **1994**, *111*, 315. (f) Haushalter, R. C.; Mundi, L. A. *Chem. Mater.* **1992**, *4*, 31.

(3) Khan, M. I.; Meyer, L. M.; Haushalter, R. C.; Schweitzer, A. L.; Zubieta, J.; Dye, J. L. *Chem. Mater.* **1996**, *8*, 43.

(4) (a) Chang, R. S.; Wang, S. L.; Lii, K. H. *Inorg. Chem.* **1997**, *36*, 3410. (b) Fan, N. Y.; Wang, S. L. *Inorg. Chem.* **1996**, *35*, 4708. (c) Wang, B.; Wang, S. L.; Lii, K. H. *Chem. Commun. (Cambridge)* **1996**, 1061. (d) Chen, T. C.; Wang, S. L. *J. Solid State Chem.* **1996**, *121*, 305. (e) Wang, S. L.; Tsai, W. J. *J. Solid State Chem.* **1996**, *122*, 36. (f) Horng, J. C.; Liao, F. L.; Wang, S. L. *Eur. J. Solid State Inorg. Chem.* **1996**, *33*, 471.

(5) (a) Lee, M. Y.; Wang, S. L. *Chem. Mater.* **1999**, *11*, 3588. (b) Hsu, K. F.; Wang, S. L. *Inorg. Chem.* **1997**, *36*, 3049. (c) Wang, S. L.; Hsu, K. F.; Nieh, Y. P. *J. Chem. Soc., Dalton Trans.* **1994**, 1681.

(6) Hsu, K. F.; Wang, S. L. *Inorg. Chem.* **1998**, *37*, 3230.

(7) Hsu, K. F.; Wang, S. L. *Chem. Mater.* **1999**, *11*, 1876.

(8) Zid, M. F.; Jouini, T. *Acta Crystallogr.* **1996**, *C52*, 1334.

(9) Zid, M. F.; Jouini, T. *Acta Crystallogr.* **1996**, *C52*, 2947.

10.1021/ic000283w CCC: $19.00
Published on Web 09/02/2000

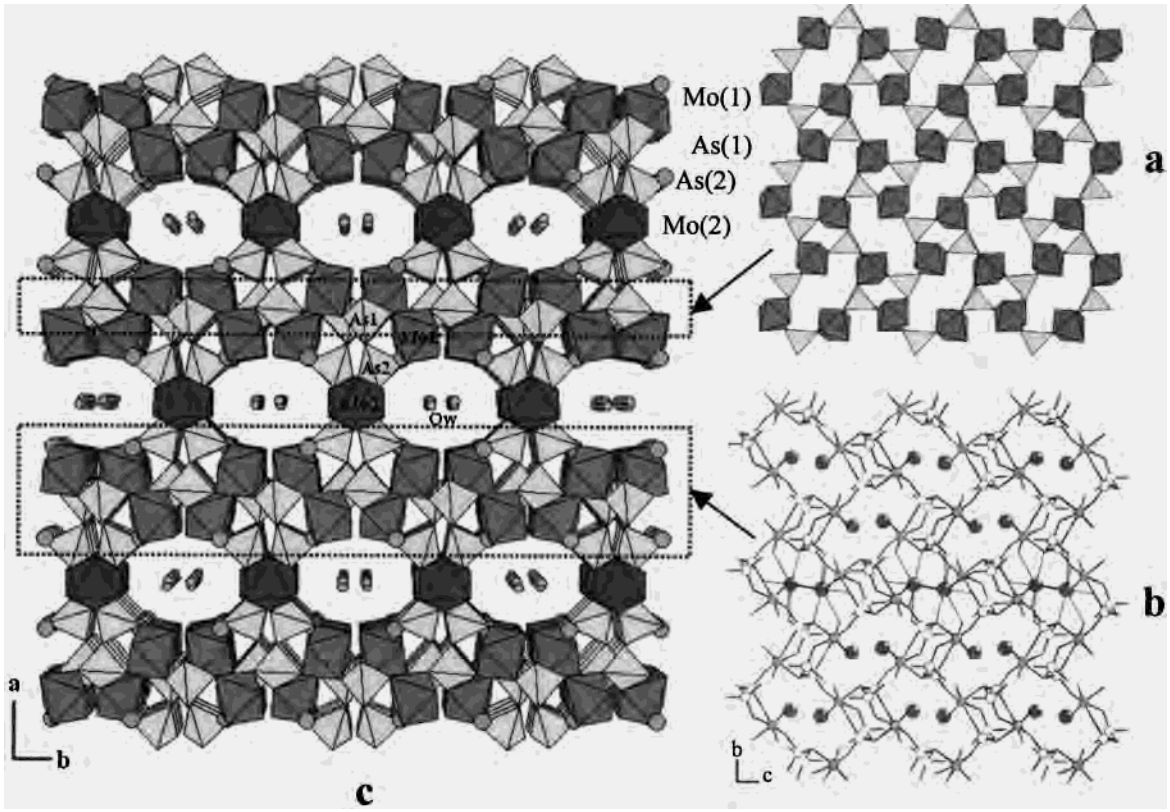

Figure 3. Schematic drawings of structure **1**: (a) section of 3-connected $^{2}_{\infty}[MoO_2AsO_4]$ layer with 4-ring and 8-ring windows; (b) section of $^{2}_{\infty}[MoO_2As_2O_7]$ porous sheets encapsulating Rb^+ cations; and (c) 3D network viewed along [001] showing elliptically shaped tunnels. Darker polyhedra: MoO_6 octahedra. Gray polyhedra: AsO_4 tetrahedra. Large circles: Rb^+ cations. Small circles: Ow atoms of water molecules.

$(MoO_2)_3(As_2O_7)_2{\cdot}2H_2O$ (**1**), a unique open-framework material with 21% solvent accessible volume and excellent thermal stability. In this paper, the synthesis, crystal structure, thermal analysis of **1**, and the structural relationship between **1** and the compositional analogue $K_2MoO_2(MoO_2As_2O_7)_2$ are presented.

Experimental Section

Synthesis and Compositional Characterization. Chemicals of reagent grade were used as received. A mixture of RbH_2AsO_4 (0.0905 g, 0.4 mmol), MoO_3 (0.0864 g, 0.6 mmol), and $NH_4H_2AsO_4$ (0.0636 g, 0.4 mmol) was ground in an agate mortar, placed in a platinum crucible (3 mL), and heated at 550 °C for 12 h, followed by a slow cooling (5 °C h^{-1}) to 400 °C and quench to room temperature on removal of the crucible from the furnance. The molten salt was then washed in boiling water, and a solid product was obtained by suction filtration. The product contained a single phase of colorless columnar crystals of $Rb_2(MoO_2)_3(As_2O_7)_2{\cdot}H_2O$ (**1**). A powder X-ray diffraction pattern of the bulk sample compared well with the pattern simulated from the coordinates of single-crystal data (vide infra). The Rb:Mo:As ratios were also confirmed by the result of electron microprobe analysis.

Single-Crystal X-ray Structure Analysis. Crystallographic data for **1** are listed in Table 1. A crystal of dimensions 0.05 × 0.08 × 0.13 mm was selected for indexing and intensity data collection. The measurements were performed on a Siemens Smart-CCD diffractometer system equipped with a normal focus, 3 kW sealed-tube X-ray source (λ = 0.71073 Å). Intensity data were collected in 1271 frames with increasing ω (width of 0.3° per frame). Unit cell dimensions were determined by a least-squares fit of 4743 reflections. Of the 2309 unique reflections (θ_{max} = 28.67°), 2130 reflections ($I > 2\sigma(I)$) were considered observed after Lorentz polarization and empirical absorption corrections. Empirical absorption correction was performed based on 3391 symmetry-equivalent reflections using the SADABS program.[10] On the basis of systematic absences and statistics of intensity distribution, the space group *C*2/*c* was determined. Direct methods were used to locate the metal and arsenic atoms with the remaining non-hydrogen atoms being found from successive difference maps. The structure was refined by full-matrix least squares based on F^2 values. Water hydrogens were not located. The final cycles of refinement, including the atomic coordinates (Table 2) and anisotropic thermal parameters for all non-hydrogen atoms, converged at R1 = 0.0353 and wR2 = 0.0904. Corrections for secondary extinction and anomalous dispersion were applied. Neutral-atom scattering factors for all atoms were taken from the standard sources. Calculations were performed on PC using *SHELXTL-Plus* programs.[11]

Thermal Analysis. Thermogravimetric analysis, using a Seiko TG/DTA 300 analyzer, was performed on a powder sample (10.4 mg) of **1** under flowing N_2 with a heating rate of 10 °C min^{-1}. In the TG/DT curves shown in Figure 1, a small amount of weight loss (2.8%) observed at ~65 °C should be attributed to the release of two water molecules (calcd 3.2%). A surge of weight loss observed beyond ~680 °C should correspond to the first evaporation of $2As_2O_3$ (calcd 35.5%), $2O_2$ (calcd 5.74%), and the final sublimation of MoO_3.[4−7] Two endothermic peaks were detected in the DT curve. The sharp one at 645 °C without a counterpart in the TG curve might correspond to a phase change right before framework decomposition. The broad peak centered at 865 °C may account for the bond-breaking process associated with the evolvement of As_2O_3 and MoO_3. To check thermal stability of the framework, a sample of **1** was then heated in a furnace at 600 °C for 4 h. Powder XRD measurements performed on the product of thermal treatment confirmed that the dehydrated form retained the same framework as **1** to 600 °C.

(10) Sheldrick, G. M. *SADABS*: *Siemens Area Detector Absorption Correction Software*; University of Göttingen: Göttingen, Germany, 1998.

(11) Sheldrick, G. M. *SHELXTL-Plus NT crystallographic system*, release 5.10; Brucker Analytical X-ray Systems: Wisconsin, 1998.

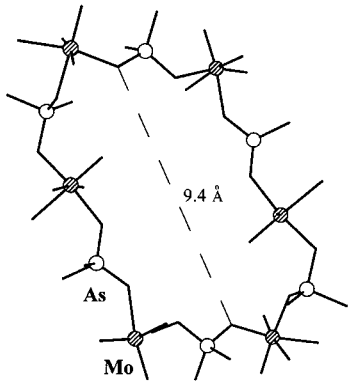

Figure 4. Ball-and-stick drawing of the puckered 12-ring window at the opening of elliptical tunnels along [001].

Table 2. Atomic Coordinates and Thermal Parameters (Å^2) for **1**

atom	*x*	*y*	*z*	U_{eq}[a]
Rb(1)	0.12453(4)	0.76856(7)	−0.37470(7)	0.0402(2)
Mo(1)	0.17923(2)	0.84464(5)	0.22897(4)	0.0167(2)
Mo(2)	0	0.55194(6)	0.25	0.0163(2)
As(1)	0.24101(2)	0.55876(5)	0.05599(5)	0.0150(2)
As(2)	0.09519(2)	0.62081(5)	0.00945(5)	0.0154(2)
O(1)	0.2919(2)	0.5328(4)	−0.0597(4)	0.0196(8)
O(2)	0.2394(2)	0.4204(4)	0.1617(4)	0.0207(8)
O(3)	0.2488(2)	0.7046(4)	0.1462(4)	0.0208(8)
O(4)	0.1645(2)	0.5507(4)	−0.0413(4)	0.0202(8)
O(5)	0.1128(2)	0.7770(4)	0.0673(4)	0.0225(8)
O(6)	0.0432(2)	0.6259(4)	−0.1374(4)	0.0194(7)
O(7)	0.0757(2)	0.5185(4)	0.1390(4)	0.0197(8)
O(8)	0.1675(2)	0.7212(4)	0.3461(5)	0.0289(9)
O(9)	0.1317(2)	0.9729(4)	0.2731(4)	0.0247(8)
O(10)	−0.0361(2)	0.6581(4)	0.1258(4)	0.0264(9)
Ow	0.0010(15)	0.9435(23)	−0.4093(31)	0.339(12)

[a] U_{eq} is defined as one-third of the trace of the orthogonalized $\mathbf{U}_{ij}$ tensor.

Results and Discussion

The asymmetric unit of **1** contains two tetrahedral centers, As(1) and As(2), sharing a common vertex to form an As_2O_7 group, and two isolated octahedral centers, Mo(1) and Mo(2), each sharing four corners with As_2O_7 groups (Figure 2). On the *bc* planes, polyhedral $Mo(1)O_6$ and $As(1)O_4$ are interlinked into 3-connected $^2_\infty[MoO_2AsO_4]$ layers with 4-ring and 8-ring windows (Figure 3a). Similar layers were previously found in the structures of $SrMoO_3HAsO_4H_2O$,[7] $A(MoO_2AsO_4)_2$ (A = Sr,[7] Ba[12]), $K_{0.17}MoP_2O_7$,[13] $AgMo_5P_8O_{33}$,[14] and $A(MoO_2)(H_2O)(PO_4)$ (A = K, NH_4).[15] The $As(2)O_4$ tetrahedra are pendent to both sides of the $^2_\infty[MoO_2AsO_4]$ layer by sharing two vertexes separately with one $Mo(1)O_6$ and one $As(1)O_4$, resulting in thick $^2_\infty[MoO_2As_2O_7]$ polyhedral sheets in which the Rb^+ cations are encapsulated (Figure 3b). The sheet is in turn linked to neighboring sheets by pillaring $Mo(2)O_6$ octahedra. Consequently, elliptically shaped tunnels are formed along the [001] direction (Figure 3c). The opening of ellipical tunnels, as depicted in Figure 4, is a puckered 12-ring window with the maximum diameter (minimum O···O distance less one O diameter of 2.8 Å) of ~9.4 Å. Free diameters of these tunnels are slightly larger than the 10-ring elliptical channels in $AlPO_4$-11.[16] In the structure of **1**, another set of tunnels with 4-ring windows can be observed in the [010] direction. Two arrays of water molecules are located at the intersections of these orthogonal tunnels. According to our thermal study, the waters of solvation can be reversibly removed while the crystallinity of the framework is maintained.

One remarkable feature of **1** is that the Rb^+ cations are confined in the cavities that are nearly embedded in the $^2_\infty[MoO_2As_2O_7]^{2-}$ sheets, resulting in tunnels dominated by small water molecules. This is opposite to typical anionic frameworks where the tunnels are filled with countercations. Neutral tunnels solely occupied by solvents normally exist in neutral frameworks and are scarcely observed in molybdenum chemistry. To our knowledge, the only example lies in the structure of $Mo_8O_{12}(PO_4)_4(HPO_4)_2 \cdot 13H_2O$,[17] a highly porous material with 35 vol % void space. On the basis of the result of PLATON analysis,[18] the title compound as well shows considerable solvent accessible volume of ~404.1 Å^3 (~21 vol %) which is not occupied by the framework Mo, As, and O atoms.

As shown in Table 3, the MoO_6 octahedron in **1** exhibits two short molybdenyl Mo=O bonds and two medium and two long Mo–O bonds which are typical for an isolated Mo^{6+} center. The

Table 3. Selected Bond Lengths (Å) and Bond Valence Sums ($\sum s$) for **1**

Rb(1)−O(9)[a]*	2.901(4)	Rb(1)−O(10)[d]	3.037(4)
Rb(1)−O(8)[b]	2.951(4)	Rb(1)−Ow	3.10(3)
Rb(1)−O(7)[c]	3.012(4)	Rb(1)−O(3)[e]	3.229(4)
Rb(1)−O(2)[c]	3.031(4)	Rb(1)−O(1)[f]	3.242(4)
$\sum s$[Rb(1)−O] = 1.14		Rb(1)−O(6)	3.314(4)
Mo(1)−O(8)	1.687(4)	Mo(1)−O(2)[g]	2.029(4)
Mo(1)−O(9)	1.694(4)	Mo(1)−O(1)[e]	2.160(4)
Mo(1)−O(5)	2.054(4)	Mo(1)−O(3)	2.225(4)
$\sum s$[Mo(1)−O] = 5.91			
Mo(2)−O(10)	1.685(4)	Mo(2)−O(7)[h]	2.045(4)
Mo(2)−O(10)[h]	1.685(4)	Mo(2)−O(6)[i]	2.187(4)
Mo(2)−O(7)	2.045(4)	Mo(2)−O(6)[j]	2.187(4)
$\sum s$[Mo(2)−O] = 5.96			
As(1)−O(1)	1.650(4)	As(1)−O(2)	1.696(4)
As(1)−O(3)	1.668(4)	As(1)−O(4)	1.754(4)
$\sum s$[As(1)−O] = 4.96			
As(2)−O(5)	1.657(4)	As(2)−O(7)	1.683(4)
As(2)−O(6)	1.663(4)	As(2)−O(4)	1.734(4)
$\sum s$[As(2)−O] = 5.05			

* Symmetry codes: (a) $x, -y+2, z-{}^1/_2$; (b) $x, y, z-1$; (c) $x, -y+1, z-{}^1/_2$; (d) $-x, y, -z-{}^1/_2$; (e) $-x+{}^1/_2, -y+{}^3/_2, -z$; (f) $-x+{}^1/_2, y+{}^1/_2, -z-{}^1/_2$; (g) $-x+{}^1/_2, y+{}^1/_2, -z+{}^1/_2$; (h) $-x, y, -z+{}^1/_2$; (i) $-x, -y+1, -z$; (j) $x, -y+1, z+{}^1/_2$.

Table 4. Mo−O Distances (Å) in Various $Mo^{VI}O_6$ Octahedra

compound	unit	Mo=O	Mo−O_m[a]	Mo−O_l[a]
$Rb_2(MoO_2)_3(As_2O_7)_2 \cdot 2H_2O$	isolated MoO_6	1.688	2.043	2.190
$Cs_2Mo_2O_5As_2O_7 \cdot H_2O$[b]	corner-shared Mo_2O_{11}	1.696	1.987	2.234
$Cs_2Mo_2O_5(HAsO_4)_2 \cdot H_2O$[c]	edge-shared Mo_2O_{10}	1.703	1.953	2.280
$Cs_5Mo_8O_{24}(OH)_2AsO_4 \cdot 2H_2O$[c]	face-shared Mo_2O_9	1.708	1.922	2.367

[a] Mo−O_m and Mo−O_l separately denote the average distances of two medium and two long Mo−O bonds. [b] Reference 6. [c] Reference 4.

(12) Masse, R.; Averbuch-Pouchot, M. T. *J. Solid State Chem.* **1985**, *58*, 157.
(13) Leclaire, A.; Borel, M. M.; Grandin, A.; Raveau, B. *J. Solid State Chem.* **1989**, *78*, 220.
(14) Lii, K. H.; Johnston, D. C.; Goshorn, D. P.; Haushalter, R. C. *J. Solid State Chem.* **1987**, *71*, 131.
(15) (a) Peascoe, R.; Clearfield, A. *J. Solid State Chem.* **1991**, *95*, 83. (b) Millini, R.; Carati, A. *J. Solid State Chem.* **1995**, *118*, 153.
(16) Richardson, J. W.; Pluth, J. J.; Smith, J. V. *Acta Crystallorg., Sect. B* **1988**, *44*, 367.
(17) Mundi, L. A.; Strohmaier, K. G.; Goshorn, D. P.; Haushalter, R. C. *J. Am. Chem. Soc.* **1990**, *112*, 8182.
(18) Spek, L. *Acta Crystallogr., Sect. A* **1990**, *46*, C34.

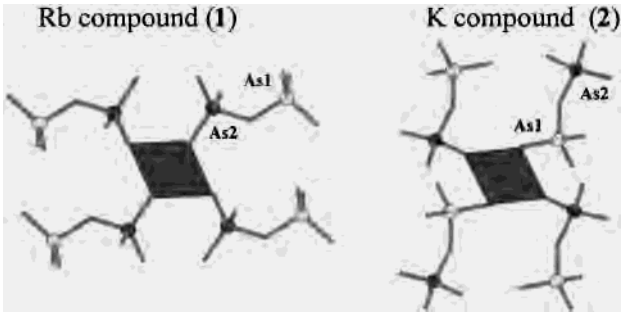

Figure 5. Alignment of As_2O_7 groups with respect to MoO_6 octahedra in $Rb_2(MoO_2)_3(As_2O_7)_2 \cdot 2H_2O$ and $K_2MoO_2(MoO_2As_2O_7)_2$. ∠As1−O−As2: 125.6° for **1** and 120.5° for **2**. Torsional angle between tetrahedra As1 and As2: 5.7° for **1** and 26.6° for **2**.

gap between the medium and the long Mo−O bonds in isolated MoO_6 octahedra is not as pronounced as those in nondiscrete $Mo^{VI}O_6$ octahedra of known cesium molybdenum(VI) arsenates (Table 4). It is noted that the title compound has the same stoichiometry and space-group symmetry as $K_2MoO_2(MoO_2As_2O_7)_2$.[9] Both adopt tunnel structures, however, in different topology due to the subtle distinction in the orientation of the diarsenate groups. As shown in Figure 5, the four As_2O_7 groups attached to the $Mo(2)O_6$ octahedra are aligned with repect to the edge of two molybdenyl oxygens in a nearly perpendicular fashion in the Rb compound whereas they are parallel in the K compound. The K^+ cations are distributed at the edges of butterfly-shaped tunnels in $K_2MoO_2(MoO_2As_2O_7)_2$. The latter framework has a higher framework-metal-atom density (16.3 M atoms/1000 Å^3) and a much lower content of void space (∼3.4 vol %) as compared with **1**.

In this work, a novel microporous molybdenum diarsenate phase, $Rb_2(MoO_2)_3(As_2O_7)_2 \cdot 2H_2O$, has been synthesized via a flux-growth method. This porous structure exhibits excellent thermal stability comparable to that of known aluminophosphate zeolites.[19] It would be interesting to prepare the corresponding phosphate analogue. Investigations along this line will be undertaken.

Acknowledgment. We are grateful to the National Science Council of the Republic of China for support of this work (NSC 89-2113-M-007 −025).

Supporting Information Available: One figure of powder X-ray diffraction patterns and four tables of complete crystal data, atomic coordinates, bond distances and angles, and anisotropic thermal parameters for **1**. This material is available free of charge via the Internet at http://pubs.acs.org.

IC000283W

(19) (a) Annen, M. J.; Yound, D.; Davis, M. E.; Cavin, O. B.; Hubbard, C. R. *J. Phys. Chem*. **1991**, *95*, 1380. (b) Yu, J.; Sugiyama, K.; Zheng, S.; Qiu, S.; Chen, J.; Xu, R.; Sakamoto, Y.; Terasaki, O.; Hiraga, K.; Light, M.; Hursthouse, M. B.; Thomas, J. M. *Chem. Mater*. **1998**, *10*, 1208.